

# Novel Structural Motifs in Clusters of Dipolar Spheres: Knots, Links and Coils

Mark A. Miller and David J. Wales

*University Chemical Laboratory, Lensfield Road, Cambridge CB2 1EW, United Kingdom*

(Dated: November 14, 2018)

We present the structures of putative global potential energy minima for clusters bound by the Stockmayer (Lennard-Jones plus point dipole) potential. A rich variety of structures is revealed as the cluster size and dipole strength are varied. Most remarkable are groups of closed-loop structures with the topology of knots and links. Despite the large number of possibilities, energetically optimal structures exhibit only a few such topologies.

PACS numbers: 36.40.Mr, 61.46.+w

Isotropic van der Waals or depletion forces favor compact packing of spherical particles, since such arrangements lead to a large number of nearest neighbor interactions. For small clusters, icosahedral motifs often prevail,<sup>1</sup> giving way to close packing for sufficiently large or bulk systems. In contrast, the energetically optimal arrangement of two purely dipolar particles is with the dipoles aligned head-to-tail, leading to chain formation. In systems with both isotropic and dipolar interactions, frustration arises from the competition between these two effects.

The study of dipolar sphere systems has a long and controversial history, concerned mostly with the existence and nature of their phase transitions.<sup>2</sup> Fresh impetus comes from recent experiments, in which nanoparticles of low polydispersity with a magnetic dipole have been synthesized and studied by electron microscopy.<sup>3</sup> Dipolar particles have also been harvested from magnetotactic bacteria.<sup>4</sup> Colloidal systems like these provide great scope for exploring the influence of particle interactions on structure and dynamics both because highly detailed information is available from electron or confocal microscopy, and because the form of the interactions can be finely tuned by the experimental conditions.<sup>5</sup>

Dipolar particles start to aggregate at low volume fractions,<sup>3</sup> producing chains and clusters. In this Letter, we identify the energetically optimal structures of clusters composed of spherical particles that interact through a permanent (electric or magnetic) dipole moment in addition to an isotropic soft core and attractive tail. We ask how the morphology of the clusters is affected by the number of particles and the strength of the dipolar interaction relative to the isotropic attraction due to van der Waals or depletion forces.

We start with the Stockmayer potential,

$$V = \epsilon \sum_{i < j}^N \left\{ 4 \left[ \left( \frac{\sigma}{r_{ij}} \right)^{12} - \left( \frac{\sigma}{r_{ij}} \right)^6 \right] + \frac{\mu^2 \sigma^3}{r_{ij}^3} \left[ \hat{\boldsymbol{\mu}}_i \cdot \hat{\boldsymbol{\mu}}_j - \frac{3}{r_{ij}^2} (\hat{\boldsymbol{\mu}}_i \cdot \mathbf{r}_{ij})(\hat{\boldsymbol{\mu}}_j \cdot \mathbf{r}_{ij}) \right] \right\},$$

for the total pairwise interaction energy of  $N$  dipolar particles, where  $\mathbf{r}_{ij}$  is the position of particle  $j$  relative to

particle  $i$  and  $\hat{\boldsymbol{\mu}}_i$  is a unit vector along the dipole moment of particle  $i$ . The units of energy and length are set by the Lennard-Jones (LJ)  $\epsilon$  and  $\sigma$  parameters, while the dimensionless parameter  $\mu$  determines the strength of the dipolar contribution relative to the LJ part.

Considerable progress has been made in the field of global optimization in the decade since Clarke and Patey first searched for the lowest energy structures of small dipolar structures using simulated annealing.<sup>6</sup> These authors concentrated particularly on the  $N = 13$  cluster, denoted here  $\text{St}_{13}$ , finding a sequence of structures with increasing  $\mu$  that has been verified recently.<sup>7</sup> For larger sizes, “intestinal” structures were reported, and the analysis of these intricate assemblies is one purpose of the present contribution. We employ the well documented basin-hopping algorithm,<sup>1</sup> in which a Monte Carlo simulation is run on a transformed potential energy surface by performing a local geometry optimization at each step. We found that geometry optimizations converged more efficiently if each  $\hat{\boldsymbol{\mu}}_i$  is represented by a pair of spherical polar angles rather than by a Cartesian vector, since the latter contains a redundant third degree of freedom.

Global optimization runs were performed for  $3 \leq N \leq 55$  particles and a grid of dipole strengths covering the range  $0 \leq \mu \leq 6$ , each run initiated from a random configuration. Starting from the optimal structure of a neighboring size is often detrimental, since the global minimum can change abruptly with  $N$  or  $\mu$ , potentially trapping the search in the wrong morphology. To prevent particles from occasionally drifting away, the cluster was placed inside a hard spherical container. The number and length of runs varied with cluster size and dipole strength as required to obtain reliably reproducible global minima. Since the dipolar contribution to the energy changes with the square of  $\mu$ , the relevant energy scale increases rapidly as one moves away from the  $\mu = 0$  LJ limit. Some care must be taken in choosing a suitable temperature  $kT$  for the basin-hopping searches, to ensure that the transformed surface is properly explored, while the global minimum structure retains significant statistical weight. We found that  $kT/\epsilon = 1 + \mu^2/5$  was a useful starting point, though other schemes were tried in cases of doubt.

Figure 1 summarizes the occurrence of the most prominent morphologies resulting from global optimization. At

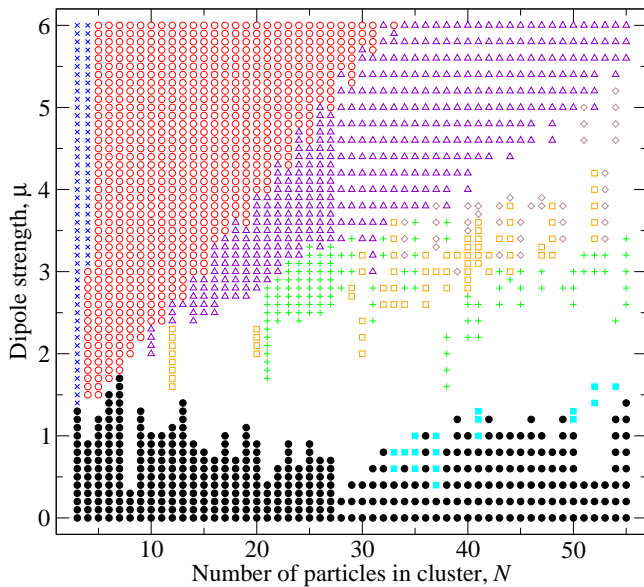


FIG. 1: Structural map for global potential energy minima of Stockmayer clusters. Symbols denote morphologies: relaxed Lennard-Jones (black filled circle), decahedral (cyan filled square), linear (blue cross), ring (red open circle), two stacked rings (purple triangle), coil (brown diamond), link (orange open square), knot (green plus). Structures that do not fall into these categories have been omitted for clarity.

$\mu = 0$ , the well known LJ structures are reproduced,<sup>1</sup> which, with the notable exception of the face-centred cubic 38-particle cluster, are constructed from icosahedral motifs. A small non-zero  $\mu$  typically leads to a slight relaxation of the LJ structure. The preference of dipoles for head-to-tail alignment gives rise to frustrated circuits of dipoles within the LJ structure, lowering the symmetry.<sup>8</sup> For example, the perfect icosahedral symmetry of the 13-atom LJ cluster is broken by loops of dipoles that point around one of the three-fold axes. Even without decorating the particles with the dipole vectors, the point group defined by the particle positions changes from  $I_h$  to  $D_3$ .

At some point, the dipole contribution to the energy becomes large enough to favor a different structure. The threshold at which the change happens varies substantially with  $N$ , depending on the nature of the competing structures. In some cases, such as  $51 \leq N \leq 54$ , a vacancy in an icosahedral shell simply finds a more favorable site. In other cases, an entirely different class of compact structures takes over, such as for certain sizes in the range  $33 \leq N \leq 41$ , where there is a switch to a decahedral motif with at least one incomplete shell. Surprisingly, the dipoles circulate roughly about an axis perpendicular, rather than parallel, to the pseudo five-fold axis. The emergence of decahedra here is partly explained by the fact that the number of nearest neighbor pairs in decahedral structures is high, relative to the underlying average, for odd  $N$  close to 38,<sup>9</sup> making decahedra competitive with icosahedra for alternate  $N$  close to this size. The exception is  $N = 39$ , where the ico-

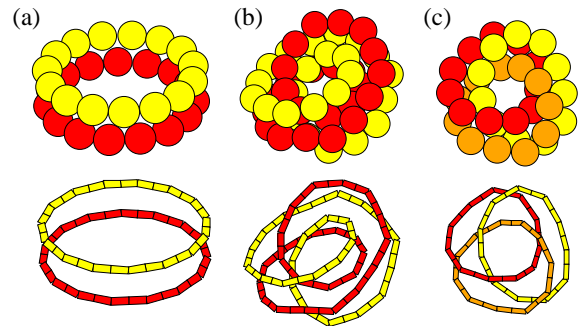


FIG. 2: Some multi-component global minima. (a)  $St_{30}$  at  $\mu = 3.6$ : the trivial unlink, (b)  $St_{48}$  at  $\mu = 3.4$ : two linked coils,  $4_1^2$ , and (c)  $St_{33}$  at  $\mu = 3.2$ : the link  $6_3^3$ . In each case, spherical particles are shown in the upper panel, and the underlying chain of dipoles in the lower. Components within each link are distinguished by color.

hedral structure has a stable partial second shell. This subtle interplay of forces is one of several examples that give rise to the diverse results mapped out in Fig. 1.

In the opposite limit of high  $\mu$ , the global minimum is a ring with the dipoles tangential to the edge for all  $N \geq 5$ . Compared with a linear structure, the energy required to bend the chain of dipoles into a ring is more than compensated by the additional contact made between the ends. When  $\mu$  is lowered sufficiently for  $N = 10$  and  $N \geq 12$ , the LJ contribution to the energy makes it more favorable to form two rings of half the size, which then stack on top of each other, creating one new nearest neighbor per particle. The threshold of  $\mu$  at which this change occurs shows an overall increase with  $N$ , since the difference in bending energy per particle between a ring of  $N$  particles and two rings of  $N/2$  particles decreases with  $N$ . For even  $N$  the two rings are planar, forming an antiprism, as illustrated in Fig. 2(a). For odd  $N$ , the two rings differ in size by one particle, and an out-of-plane distortion is necessary to accommodate the mismatch. Since some of the dipole-dipole interactions are frustrated in this arrangement, the single ring becomes more favorable at a lower  $\mu$  for odd  $N$  than for neighboring even  $N$ . The odd-even alternation in the boundary between one and two rings is clearly visible in Fig. 1.

The antiprismatic structure in Fig. 2(a) shows two clearly defined closed circuits of dipoles. While neighbors in the same chain approach somewhat more closely than members of different rings, making it possible to define chains using a distance criterion for neighbors, it is much less ambiguous to use an energetic definition. The anisotropy of the dipolar potential means that the propensity of a particle for “bonding” is effectively saturated by two particles with roughly aligned dipoles positioned at its head and tail. Starting from a given particle  $i$ , we define the next member of the chain as the particle  $j$  that has the lowest dipole-dipole interaction energy with  $i$  and is located in the half-space to which the dipole of  $i$  points, i.e.  $\hat{\mu}_i \cdot \mathbf{r}_{ij} > 0$ . The previous particle in the

chain is likewise the particle with lowest interaction energy that also satisfies  $\hat{\boldsymbol{\mu}}_i \cdot \mathbf{r}_{ij} < 0$ . This parameter-free definition reliably and intuitively decomposes a structure into its constituent chains. In compact clusters, where the dipole–dipole interactions are not dominant enough for the structure to be naturally decomposed into chains, an attempt to define chains in this way will result in a collection of meaningless fragments and can be discarded as irrelevant.

Analysis of structure in terms of chains allows us to make sense of the intermediate  $\mu$  regime, where neither the isotropic LJ energy nor the dipolar contribution dominates. One unexpected solution to the frustration between ring formation and condensation is illustrated in Fig. 3(a). In this  $St_{38}$  cluster, all the particles belong to a single closed-loop chain, but the chain has the topology of a non-trivial knot; it cannot be unravelled into a simple ring without breaking the chain. At every point in the knot, three portions of the chain are in close proximity, giving a large number of nearest neighbor interactions (114 pairs, based on a distance threshold of  $1.35\sigma$ ). At the same time, the structure remains open, limiting the bending energy, and keeping unfavorable combinations of dipole orientations apart. The  $St_{38}$  example has  $D_2$  point group symmetry, i.e. three distinct  $C_2$  rotation axes but no mirror planes. Although the projection may be unfamiliar, the structure is a trefoil, the simplest non-trivial knot, and is written  $3_1$  in Rolfsen’s notation,<sup>10</sup> meaning the first (in fact, only) knot whose reduced projection has three crossings.

The topology of a closed-loop chain is invariant to any deformation (ambient isotopy) that does not break the chain. In contrast, the occurrence of the trefoil as a global potential energy minimum clearly relies on the detailed arrangement of the particles. Nevertheless, it is natural to ask how prevalent the trefoil is, and whether knots of different topology also arise. A reliable way to distinguish prime knots is through their Jones polynomials,<sup>11</sup> which are invariant to ambient isotopies and unique for knots of up to nine crossings, as well as most of ten. We find the Jones polynomial of a knot cluster starting from an arbitrary projection of the underlying chain onto two dimensions. The so-called bracket polynomial is first derived by considering all combinations of splits at the crossings in the projection, and is then combined with a factor depending on the writhe to give the Jones polynomial.<sup>12,13</sup> The corresponding Rolfsen notation<sup>10</sup> can then be looked up in tables.<sup>11,13</sup>

The trefoil knot, of which Fig. 3(a) is an example, first appears at  $N = 21$ , though it is necessarily more compact at these smaller sizes. This topology dominates the first band of knots visible in Fig. 1 in the range  $21 \leq N \leq 38$ . However, towards the larger end of this range, a second topology,  $5_1$ , of greater complexity appears. Figure 3(b) shows that this class of global minimum is more compact than the larger trefoils. It has three neatly stacked turns, with a thread through the central axis. The significant bending of the dipole chain is compensated by

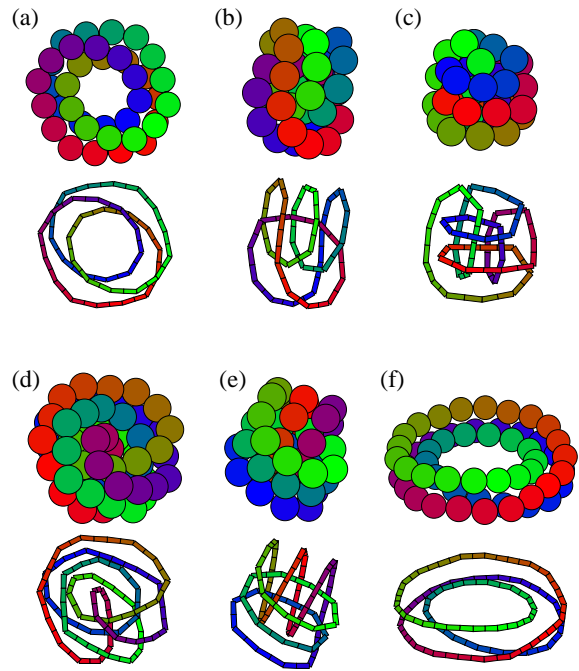


FIG. 3: (a)  $St_{38}$  at  $\mu = 3.6$ : the trefoil knot  $3_1$ , (b)  $St_{35}$  at  $\mu = 2.8$ : knot  $5_1$ , (c)  $St_{38}$  at  $\mu = 1.6$ : knot  $8_{19}$ , (d)  $St_{55}$  at  $\mu = 3.2$ : knot  $10_{124}$ , (e)  $St_{45}$  at  $\mu = 2.6$ : knot  $10_{139}$ , (f)  $St_{54}$  at  $\mu = 4.6$ : a coil with the topology of the trivial knot. In each case, spherical particles are shown in the upper panel, and the underlying chain of dipoles in the lower. The color changes smoothly along the chain.

the compactness of the overall structure.

Figure 1 shows a second band of knots, starting at lower  $\mu$  and rising with  $N$  in the range  $38 \leq N \leq 55$ . The trefoil does not occur here, but the  $5_1$  knot is a common feature. We also observe two substantially more intricate knots whose reduced projections contain ten crossings. Fortunately, despite having more than nine crossings, neither has an ambiguous Jones polynomial,<sup>14</sup> allowing both to be identified as described above. As shown in Fig. 3(e), one of them,  $10_{139}$ , resembles the  $5_1$  knot in its packing. The slightly wider turns now accommodate two threads, creating two stacks each of three turns. In the illustrated case of  $St_{45}$ , the stacks are equivalent, being interchanged by a  $C_2$  operation. The other 10-crossing knot,  $10_{124}$ , shown in Fig. 3(d), more closely resembles the twisted wreath of the trefoil in Fig. 3(a), but with a denser bundle of four turns.

A knot with eight crossings in the reduced projection,  $8_{19}$ , shown in Fig. 3(c), makes an appearance at  $N = 38$  for values of  $\mu$  below those that produce the trefoil at the same  $N$ . The smaller dipole moment means that the isotropic LJ contribution is more influential, and this cluster is indeed compact, having 156 nearest neighbor pairs, compared with 114 for the trefoil. These contacts come at the expense of some sharp bends in the chain of dipoles.

We note that it is possible for a closed chain of dipoles

to possess multiple turns without passing through its own loops to produce a knot. Such coiled structures are also observed as global minima, as illustrated by the  $St_{54}$  cluster in Fig. 3(f). Furthermore, there is the possibility of forming more than one closed chain in the same structure. Such combinations are known as links, and we have already seen a topologically trivial example in Fig. 2(a). However, non-trivial links are also encountered in the structural map of Fig. 1. The smallest and simplest example is the Hopf link,  $2_1^2$ , of two interlocked rings, which first occurs for  $St_{12}$  in the range  $1.6 \leq \mu \leq 2.3$  and consists of two interlocked hexagons. A less clear example is illustrated in Fig. 2(b) for  $St_{48}$ , which is composed of two interlocking coils, each of two turns, and has overall  $C_2$  symmetry. One three-component link topology,  $6_3^3$ , consisting of three mutually interlocked rings, has also been observed, and is illustrated in Fig. 2(c). The interplay of factors that determine the number of components in a link is expected to be rather delicate, and indeed  $St_{33}$  is a  $6_3^3$  link for values of  $\mu$  where  $St_{32}$  or  $St_{34}$  is a knot. In this case the balance may be tipped by the fact that the 33-particle cluster can be divided into three rings of equal size.

The occurrence of such topologically exotic structures as global minima of the simple model Stockmayer potential was unexpected. On the other hand, given that knots turned out to be optimal in some cases, it is now remarkable that only a few topologies are observed for  $N \leq 55$  out of the 249 possibilities with up to ten crossings. For larger clusters, where a single closed-loop chain would be long enough to accommodate even more crossings, the possibility of yet more complex topologies arises.

However, the present identification by Jones polynomials would then be inadequate, since the polynomials are not unique for 10 or more crossings.<sup>14</sup> For sufficiently strong dipole moment, the global minimum of a large cluster will always be a ring to obtain the maximum number of head-to-tail contacts. However, as Fig. 1 shows, the threshold at which rings are optimal increases with size. In contrast, the average dipole strength at which the LJ structure is superseded shows no overall trend with size. The range of dipole strengths over which complex structures such as knots may be found therefore widens with increasing cluster size.

The fact that knots appear over a reasonable spread of sizes and dipole strengths suggests that there is a good chance of observing some of them experimentally in suspensions of dipolar colloids. However, while the advantages of the Stockmayer potential include being well known, the LJ contribution is only one choice for the isotropic attraction. For some colloids, a shorter-range potential and stiffer repulsive core might be more appropriate, and it would be interesting to see whether the delicate balance of nearest-neighbor and chain-like tendencies that leads to knots is preserved with respect to such changes.

A number of other questions arise concerning thermodynamic stability at finite temperature, and the mechanism and dynamics of self-assembly.<sup>15</sup> Further work is required to relate these properties to the overall organization of the underlying potential energy landscape.<sup>16</sup>

MAM is grateful to Churchill College, Cambridge for financial support.

---

<sup>1</sup> Wales, D. J.; Doye, J. P. K. *J. Phys. Chem. A* **1997**, *101*, 5111–5116.  
<sup>2</sup> Teixeira, P. I. C.; Tavares, J. M.; Telo da Gama, M. M. *J. Phys. Cond. Matt.* **2000**, *12*, R411–R434.  
<sup>3</sup> Butter, K.; Bomans, P. H. H.; Frederik, P. M.; Vroege, G. J.; Philipse, A. P. *Nature Materials* **2003**, *2*, 88–91.  
<sup>4</sup> Philipse, A. P.; Maas, D. *Langmuir* **2002**, *18*, 9977–9984.  
<sup>5</sup> Frenkel, D. *Science* **2002**, *296*, 65–66.  
<sup>6</sup> Clarke, A. S.; Patey, G. N. *J. Chem. Phys.* **1994**, *100*, 2213–2219.  
<sup>7</sup> Oppenheimer, C. A.; Curotto, E. *J. Chem. Phys.* **2004**, *121*, 6226–6239.  
<sup>8</sup> Lavender, H. B.; Iyer, K. A.; Singer, S. J. *J. Chem. Phys.* **1994**, *101*, 7856–7867.  
<sup>9</sup> Doye, J. P. K.; Wales, D. J. *Chem. Phys. Lett.* **1995**, *247*,

339–347.  
<sup>10</sup> Rolfsen, D. *Knots and Links*; Publish or Perish Press: Berkeley, 1976.  
<sup>11</sup> Jones, V. F. R. *Bull. Amer. Math. Soc.* **1985**, *12*, 103–111.  
<sup>12</sup> Lickorish, W. B. R.; Millett, K. C. *Mathematics Magazine* **1988**, *61*, 3–23.  
<sup>13</sup> Adams, C. C. *The Knot Book*; American Mathematical Society: Providence, 2004.  
<sup>14</sup> Jones, V. F. R. *Ann. Math.* **1987**, *126*, 335–388.  
<sup>15</sup> van Workum, K.; Douglas, J. F. *Phys. Rev. E* **2005**, *71*, 031502.  
<sup>16</sup> Wales, D. J. *Energy Landscapes*; Cambridge University Press: Cambridge, 2004.